Cancer Letters 459 (2019) 100–111

Contents lists available at ScienceDirect

Cancer Letters

journal homepage: www.elsevier.com/locate/canlet

Original Articles

# MLKL attenuates colon inflammation and colitis-tumorigenesis via suppression of inflammatory responses

Qun Zhao[a,b,1], XianJun Yu[b,1], Ming Li[a], YongBo Liu[a], YaMei Han[a], XiXi Zhang[a], Xiao Ming Li[a], XiaoXia Wu[a], Jun Qin[c], Jing Fang[a], Haibing Zhang[a,*]

[a] CAS Key Laboratory of Nutrition, Metabolism and Food Safety, Shanghai Institute of Nutrition and Health, Shanghai Institutes for Biological Sciences, University of Chinese Academy of Sciences, Chinese Academy of Sciences, Shanghai, 200031, China
[b] Laboratory of Inflammation and Molecular Pharmacology, School of Basic Medical Sciences & & Biomedical Research Institute, Hubei University of Medicine, Shiyan, 442000, China
[c] CAS Key Laboratory of Tissue Microenvironment and Tumor, CAS Center for Excellence in Molecular Cell Science, Shanghai Institute of Nutrition and Health Sciences, Shanghai Institutes for Biological Sciences, Chinese Academy of Sciences, University of Chinese Academy of Sciences, Shanghai, 200031, China

ARTICLE INFO

*Keywords:*
MLKL
Necroptosis
Dendritic cells
Colitis-associated tumorigenesis

ABSTRACT

The mixed lineage kinase domain-like protein (MLKL) has emerged as a critical mediator of necroptosis, which results in the release of cellular damage-associated molecular patterns (DAMPs). However, its physiological role in regulating inflammation is not fully understood. We herein showed that *Mlkl*$^{-/-}$ mice were highly susceptible to colitis and colitis-associated tumorigenesis (CAT), which was associated with massive leukocyte infiltration and increased inflammatory responses. Moreover, we used bone marrow transplantation to reveal that MLKL in inflammatory cells is crucial for its role on colitis. Intestinal mucosal tissue and polyps isolated from *Mlkl*$^{-/-}$ mice exhibited increased ERK activation and elevated expression of genes associated with inflammation and cancer. Mechanistically, enhanced inflammation in *Mlkl*$^{-/-}$ mice was due to MEK/ERK activation particularly in dendritic cells (DCs). Our results demonstrate the role of MLKL in maintaining intestinal homeostasis and protecting against colitis and tumorigenesis.

## 1. Introduction

The innate immune system provides first-line defenses against endogenous danger signals and invading microbial organisms [1]. Although inflammation is a host protective response against infection and injury, excessive inflammation is thought to be due to chronic tissue damage and tumor initiation and progression [2,3]. Colorectal cancer is one of the leading causes of death worldwide [4,5]. Inflammatory bowel disease (IBD), comprising ulcerative colitis and Crohn's disease, is associated with an increased the risk of colorectal cancer [6–8]. Ulcerative colitis is an immune-mediated disorder, leading to invasion of colonic commensal microflora and mucosal immune cells [9,10]. Although the mechanisms have not been completely elucidated, recent studies have demonstrated that excessive range of cytokines, chemokines and growth factors produced during chronic inflammation appear to be key triggers in the pathogenesis of experimental colitis and development of IBD in humans [11,12].

Chronic inflammatory diseases of the gut result from the aberrant interaction between the host immune system and commensal microflora [9]. Innate immune receptors, such as Toll-like receptors (TLR) and tumor necrosis factor receptors (TNFR), initiate the inflammatory process and regulate proinflammatory cytokine and chemokine production in epithelial cells and immune cells through the nuclear factor-κB (NF-κB) and mitogen-activated protein kinase (MAPK) signaling pathways [13]. Notably, tight regulation of these signaling pathways is critical for maintaining intestinal homeostasis [14–16]. In addition, recent evidence suggest a critical role for signal transducer and activator of transcription family proteins (STATs), especially STAT3, in the co-regulation of numerous oncogenic and inflammatory genes with NF-κB [17–19]. The MAPK pathways, including extracellular signal-regulated kinase 1/2 (ERK1/2), the Jun N-terminal kinase (JNK) and p38 pathways, are often dysregulated in inflammatory and cancer [20,21]. Both NF-κB and MAPKs signaling pathways can regulate cyclooxygenase-2 (COX-2) expression, an enzyme expressed in the intestine and required for the maintenance of intestinal homeostasis, leading to production of prostaglandin E2 (PGE2) and arachidonic acid [22].

* Corresponding author.
*E-mail address:* hbzhang@sibs.ac.cn (H. Zhang).
[1] Co-first author.

https://doi.org/10.1016/j.canlet.2019.05.034
Received 8 January 2019; Received in revised form 23 May 2019; Accepted 24 May 2019

Therefore, deregulation of these mediators may represent a key mechanism contributing to colon inflammation, colitis and colorectal tumorigenesis.

Necroptosis is a type of cell death induced by the tumor necroptosis factor superfamily and other extracellular and intracellular stimuli in certain pathologies. Receptor-interacting protein kinase 1 (RIPK1) and RIPK3 are critical adaptors of necroptosis [23–25]. RIPK1 and RIPK3 interact via the RIP homotypic interaction motif (RHIM) domains and form the necrosome [26]. As a substrate of RIPK3, MLKL is phosphorylated by RIPK3, oligomerizes, and then translocates to the cell membrane, resulting in the release of cellular contents promoting inflammation [27,28]. Necroptosis plays an important role in aggravated chronic inflammatory diseases such as atherosclerosis and cerulein-induced acute pancreatitis [29–31]. However, the consequences of necroptosis are not necessarily proinflammatory. Recent evidence suggests that, under certain conditions, necroptosis can suppress inflammation via decreasing inflammatory production and enhancing pathogen clearance, leading to inhibition of inflammatory responses [32]. More recently, *Ripk3*$^{-/-}$ mice have been shown to be more susceptible to colon inflammation in response to injury and colitis-associated colon cancer [33,34]. Although MLKL is considered to be downstream of RIPK3 in necroptosis signaling, our findings and studies conducted by others have demonstrated the observed differences between *Ripk3*$^{-/-}$ and *Mlkl*$^{-/-}$ mice [35,36]. Interestingly, low MLKL expression was previously shown to be associated with poor prognosis in colorectal cancer and administration of MLKL mRNA inhibited tumor growth [37,38]. However, the role of MLKL in the pathogenesis of colon inflammation and tumorigenesis remains unclear and needs to be further characterized.

In this study, our results demonstrate that *Mlkl*$^{-/-}$ mice were highly susceptible to colitis and CAT. These phenotypes are associated with hyperactivation of innate immune responses in *Mlkl*$^{-/-}$ mice. Increased inflammatory-cytokine expression is ensured by hyper-activation of MEK/ERK in *Mlkl*$^{-/-}$ BMDCs, but not in *Mlkl*$^{-/-}$ BMDMs. Moreover, defective necroptosis does not affect the cytokine expression in *Mlkl*$^{-/-}$ BMDCs. Overall, our study indicates that MLKL exerts a protective role against DSS-induced colitis and CAT.

## 2. Materials and methods

### 2.1. Human samples

A commercial colorectal cancer cDNA was purchased from the Shanghai Outdo Biotech Co., Ltd. (Shanghai, China)). These samples were used for Real-time PCR.

### 2.2. Mice

*Mlkl*$^{-/-}$ mice has been described previously [36]. *Mlkl*$^{-/-}$ mice were originally generated on C57BL/6 background. WT and *Mlkl*$^{-/-}$ mice were housed in a specific pathogen-free facility and male mice generally used between 8 and 10 weeks of age. All animal experiments were conducted in accordance with the guidelines of the Animal Care and Use Committee of Shanghai Institute of Nutrition and Health, Shanghai Institutes for Biological Sciences, Chinese Academy of Sciences (CAS).

### 2.3. Induction of colitis

For the DSS-induced acute colitis model, WT and *Mlkl*$^{-/-}$ mice were fed with 3% (w/v) DSS (molecular mass 36–40 kDa; MP Biologicals) dissolved in sterile water for 6 days. For survivals model, colitis was induced with 3% (w/v) DSS during 6 days, followed by normal drinking water until the end of the experiment. The DSS solutions were made fresh on day 3. Body weight, stool consistency, morbidity, and occult blood in the stool were recorded daily. Disease activity index (DAI) was assessed by an investigator blinded to the experiment according to a combined score method [39]. On the last day, mice were sacrificed, then blood were collected and the colons were resected, flushed with PBS, opened longitudinally, and measured. Then the colons were collected for H&E staining and further analysis.

### 2.4. Induction of colitis-associated tumorigenesis

For the early stages of tumor induction model, WT and *Mlkl*$^{-/-}$ mice were first i.p. injected with AOM (Sigma) at 10 mg/kg body weight. After 5 days, the mice were fed with 3% (w/v) DSS in drinking water during 5 days, followed by normal drinking water until the end of the experiment on the indicated days. For the colitis-associated tumorigenesis (CAT) model, WT and *Mlkl*$^{-/-}$ mice were first i.p. injected with AOM (Sigma) at 10 mg/kg body weight. After 5 days, the mice were fed with three cycle of 3% (w/v) DSS in drinking water during 5 days, followed by normal drinking water for 2 weeks. Similar set of analyses were done as in the DSS colitis experiments. Final tumor load and tumor size were measured.

### 2.5. Cytokine assay

Whole colon was homogenized in RIPA lysis buffer containing a cocktail of protease inhibitors. Blood serum were collected. The concentration of mouse cytokines was measured by commercial ELISA kits for mouse IL-6, TNF-α and IL-1β (eBioscience), following the manufacturer's instructions.

### 2.6. Cell culture

Bone marrow cells from flushed tibias and femurs were lysised by the ACK lysis buffer to remove red blood cells. For BMDMs, bone marrow cells were differentiated for 7 days in 1640 containing 10% fetal calf serum and 50 ng/ml M-CSF (Life technologies). For BMDCs, bone marrow cells were cultured in RPMI1640 media supplemented with 10% FBS, 2 mM Glutamine, 10 ng/ml GM-CSF (BioLegend) for 5 days to differentiate into DCs. BMDMs and BMDCs were seed in 12-well plates, cultured overnight and stimulated with LPS (Sigma) and Poly I:C (Sigma).

### 2.7. Real-time quantitative PCR

About 0.5 cm of tissues from the middle ileum, proximal colon, and distal colon were sampled. Fecal contents were removed gently and rinsed with sterilized PBS. Then the tissues were ground by pestle and mortar with liquid $N_2$. For Total RNA was extracted using Trizol reagent (Life Technologies), according to the manufacturer's instructions. Cells were harvested at different time points, washed with PBS and lysates with Trizol reagent. RNA was quantified, then 1 μg total RNA was reverse transcribed to complementary DNA (TAKARA). Transcript levels of indicated cytokines were quantified by quantitative RT-PCR on an ABI 7500 real-time PCR instrument with SYBR Green. Relative expression was calculated using L32 as an internal control as indicated.

### 2.8. Western blotting

Cells were harvested at different time points, washed with PBS and lysates with 1 × SDS sample buffer containing 100 mM DTT and boiled 5 min at 95 °C. For mouse tissue protein extraction, colon tissues were ground by pestle and mortar with liquid $N_2$ and the protein was extracted with RIPA lysis buffer [40]. The lysates were cleared by centrifugation for 20 min at 13 200 × *g*, quantified by BCA kit (Thermo Fisher) then mixed with SDS sample buffer and boiled at 95 °C for 5 min. The samples were separated using SDS-PAGE, transferred to PVDF membrane (Millipore) with 100v for 2 h. The proteins were detected by using a chemiluminescent substrate (Thermo Fisher). The

indicated antibodies were used for Western blot analysis.

### 2.9. Immunohistology

Immunohistochemical staining was performed on formalinxed paran-embedded tissues using the indicated antibody. The corresponding secondary antibodies were obtained from Vector Laboratories.

### 2.10. Statistical analysis

The data are presented as the mean ± SEM of three independent experiments unless otherwise noted. The statistical comparisons between the different treatments were determined by Student's *t*-test. We also use the Two-way ANOVA with Sidak's post-test. GraphPad Prism 5.0 software was used for data analysis.

## 3. Results

### 3.1. *Mlkl*$^{-/-}$ mice are hypersusceptible to DSS-induced colitis

Previous studies have demonstrated that MLKL functions as a key regulator of the necroptotic cell death pathway [27,29,41]. Our previous findings and studies conducted by others have demonstrated that MLKL is expressed in spleen, thymus, colon, intestine, liver, and lung, whereas expression in other tissues is considerably reduced [29,35,36]. To determine the role of MLKL in regulating inflammatory responses, we crossed heterozygous *Mlkl* $^{+/-}$ mice to generate *Mlkl*$^{-/-}$ mice (SFig. 1A). WT and *Mlkl*$^{-/-}$ mice were backcrossed to the C57BL/6 genetic background for 10 generations. Homozygous *Mlkl*$^{-/-}$ mice were viable, healthy, and fertile and did not display any gross physical or behavioral abnormalities (SFig. 1B–D) Western blot using a specific antibody detected MLKL protein in spleen, lymph nodes, liver, lung and colon in WT, *Mlkl*$^{+/-}$and *Mlkl*$^{-/-}$ mice (SFig. 1E). Similarly, the absence of MLKL protein was noted in bone marrow-derived macrophages (BMDMs) and bone marrow-derived dendritic cells (BMDCs) (SFig. 1F). Tissue sections stained with H&E revealed no morphological abnormalities in liver, spleen, lung, kidney and colon between WT and *Mlkl*$^{-/-}$ mice (SFig. 1G), suggesting no significant abnormalities in the development of *Mlkl*$^{-/-}$ mice.

DSS-induced colitis model is considered model used to monitor inflammation and disruption of colonic homeostasis [42]. To address the physiological function of MLKL in colitis-induced inflammation, WT and *Mlkl*$^{-/-}$ mice were fed 3% DSS for 6 days in drinking water. Expression of both MLKL mRNA and protein were increased in the colon tissue during colitis (SFig. 1H and I). Weight loss, clinical severity and colonic shortening are considered clinical symptoms of colitis. Notably, *Mlkl*$^{-/-}$ mice exhibited increased body weight loss and clinical severity (Fig. 1A and B). Shorter colon lengths were observed in *Mlkl*$^{-/-}$ mice compared with WT mice at day 6 after DSS treatment (Fig. 1C and D). Consistent with an inflammatory phenotype, we observed enlarged spleens and mesenteric lymph nodes (mLN) in DSS-fed *Mlkl*$^{-/-}$ mice compared with WT mice (Fig. 1E and F).

To further validate excessive inflammation in *Mlkl*$^{-/-}$ mice, colon sections were subject to hematoxylin & eosin (H&E) staining. Colons of DSS-fed *Mlkl*$^{-/-}$ mice exhibited severe inflammation compared with WT mice, including increased destruction of the colonic epithelial structure and crypt loss, a larger inflamed region, and a thicker muscularis layer (Fig. 1G). Semi-quantitative scoring further confirmed that colitis severity in *Mlkl*$^{-/-}$ mice was significantly increased compared with WT mice (Fig. 1H). To assess the contribution of MLKL in the acute colitis model, mice were challenged with 3% DSS in drinking water for 6 days followed by regular drinking water for an additional 6 days. Survival was monitored until day 12 after the start of DSS (SFig. 1J). In total, 90% of *Mlkl*$^{-/-}$ mice died during the DSS administration period, but the mortality rate was less than 30% in WT mice (Fig. 1I). These results suggest that MLKL plays a protective role against DSS-induced acute colitis and mortality.

### 3.2. Increased CAT in *Mlkl*$^{-/-}$ mice

Colitis is a driver factor for colon tumorigenesis [3]. The observation that *Mlkl*$^{-/-}$ mice suffered from colorectal inflammation upon DSS treatment, prompted us to determine the role of MLKL in the initiation and progression of inflammation-driven CAT. Expression of MLKL was increased in colon tumor compared with adjacent tissue (SFig. 2A). In addition, expression of MLKL mRNA and protein were increased in azoxymethane (AOM)/DSS-induced colon cancer (SFig. 2B–D). To address the role of MLKL in CAT, WT and *Mlkl*$^{-/-}$ mice were subjected with AOM-DSS treatment. *Mlkl*$^{-/-}$ mice exhibited a drastic reduction in body weight and significantly increased clinical severity compared with WT mice (Fig. 2A), and exhibited significantly increased clinical severity in comparison with WT mice (Fig. 2B). Consistent with these clinical features, colons obtained from AOM/DSS-treated *Mlkl*$^{-/-}$ mice were markedly shorter than control mice during disease progression (Fig. 2C). In addition, *Mlkl*$^{-/-}$ mice (8/15 53.3%) demonstrated a significantly increased risk of mortality compared with WT mice (3/15 20%) in the AOM/DSS-induced CAT model (Fig. 2D). These results suggest that MLKL functions as a defense mechanism during AOM/DSS induction.

*Mlkl*$^{-/-}$ mice exhibited increased colon inflammation in the DSS model, suggesting the role of MLKL in AOM/DSS-induced colonic tumorigenesis. *Mlkl*$^{-/-}$ mice exhibited increased polyps in the anus compared with WT mice after AOM/DSS treatment (Fig. 2E and F). Consistently, increased tumor burdens were observed in the colon (Fig. 2G), and increases in the number and size of tumors were also observed in *Mlkl*$^{-/-}$ mice compared with WT mice (Fig. 2H). Previous evidence has indicated that the inflammation, crypt atrophy, hyperplasia and dysplasia scores in the colon are highly associated with tumorigenesis [13]. Based on histological examination, we observed markedly increased histopathological changes in *Mlkl*$^{-/-}$ mice compared with WT mice (Fig. 2I and J). These changes were characterized by a significant increase in inflammation, hyperplasia, and dysplasia (SFig. 2E). There results further confirm that MLKL attenuates colon tumorigenesis and suppresses the progression of colitis-associated colon cancer.

### 3.3. Exacerbated immune responses in *Mlkl*$^{-/-}$ mice during DSS exposure

The above results promoted us to investigate whether *Mlkl* deficiency in inflammatory response had a role in the pathogenesis of colitis and colitis-induced colon cancer. To address this possibility, we generated early stages of the tumor induction models (SFig. 3A). As expected, *Mlkl*$^{-/-}$ mice exhibited significantly increased body weight loss, higher rectal bleeding, and more colon shortening compared with the WT mice during early stages of tumor induction (SFig. 3B–E). Further histological examinations of colon sections revealed higher histology scores at day 5 after drinking water (Fig. 3A and B), including significantly increased severe colon inflammation, ulceration and hyperplasia in *Mlkl*$^{-/-}$ mice (SFig. 3F). Immune cell infiltration in colon tissue was then analyzed by histochemical staining. Interestingly, we observed increased infiltration of macrophages (F4/80), PMN (Gr-1) and DC (CD11c) cells in inflamed colon sections of *Mlkl*$^{-/-}$ mice (Fig. 3C **and** SFig. 3G). Similar to DSS-treated *Mlkl*$^{-/-}$ mice, splenomegaly was also apparent in early colon cancer of *Mlkl*$^{-/-}$ mice after AOM/DSS induction (SFig. 3H and I), suggesting that the progress of CAT was associated with dysregulating immune cell activation and inflammatory responses.

To further address the immune cell types associated with the hyperinflammatory responses, myeloid cells in the spleens and mLN were analyzed by flow cytometry at different stages of early tumor induction models. Consistent with the severity of colon inflammation, severe

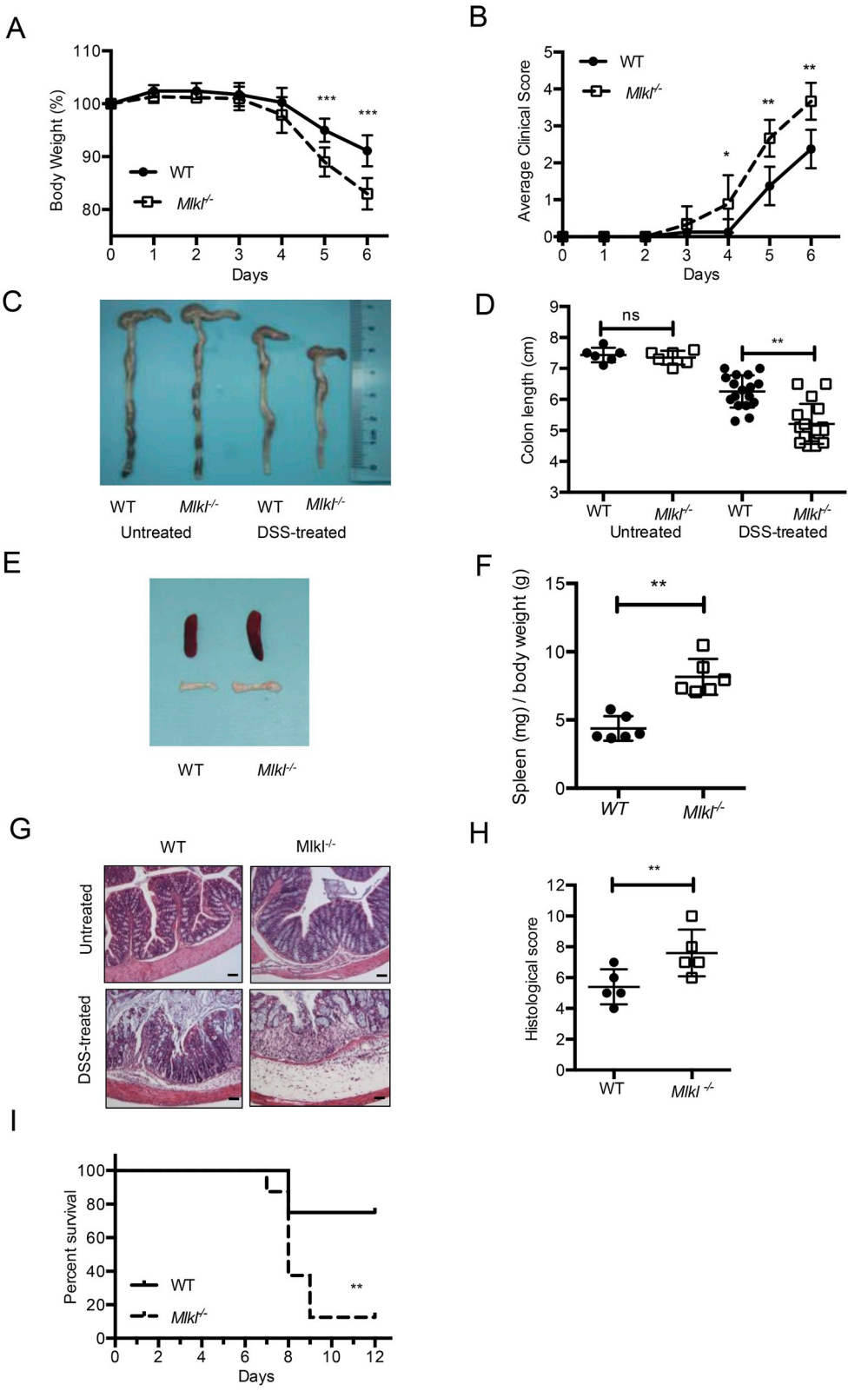


**Fig. 1. *Mlkl*$^{-/-}$ mice are hypersusceptible to DSS-induced colitis.** (A) WT (n = 8) and *Mlkl*$^{-/-}$ (n = 9) mice were fed 3% DSS for 6 days. Body weights are shown at indicated days as percent change from day 0.(B) Average clinical scores were scored daily. (C–D) WT (n = 17) and *Mlkl*$^{-/-}$ (n = 17) were sacrificed on day 6 to measure colon length. WT mock, n = 6; *Mlkl*$^{-/-}$ mock, n = 6. (E) Representative macroscopic images of spleens and mLNs of WT (n = 6) and *Mlkl*$^{-/-}$ (n = 6) mice fed DSS for 6 days. (F) Spleens weight from WT and *Mlkl*$^{-/-}$ mice collected after DSS treatment. (G) Representative microscopic images of H&E staining of colon section after DSS administration (WT, *Mlkl*$^{-/-}$, n = 5).(H) Semiquantitative scoring of histopathology. (I) Kaplan-Meier plot of WT and *Mlkl*$^{-/-}$ mice survival. WT (n = 8) and *Mlkl*$^{-/-}$ (n = 8) mice were fed 3% DSS in drinking water for 6 days. Survival was monitored until day 12 after DSS administration. For all experiments, data shown are representative of at least three independent experiments. The symbols *, **and *** indicate $p < 0.05$, $p < 0.01$ and $p < 0.001$, respectively, between the DSS-treated WT and *Mlkl*$^{-/-}$ mice.

lymphadenopathy and splenomegaly and an increases in myeloid cell types (CD11b$^{+}$, F4/80$^{+}$, CD11c$^{+}$, Gr-1$^{+}$) were observed in *Mlkl*$^{-/-}$ mice compared with WT mice at days 5 and 12 (Fig. 3D and E). Notably, at the later stage of day 20, no difference in weight loss between WT and *Mlkl*$^{-/-}$ mice was observed (SFig. 3B and C), but *Mlkl*$^{-/-}$ mice still exhibited even greater spleen and LN enlargement (SFig. 3H and I), and a larger population of myeloid cells compare with WT mice (Fig. 3D and E). Notably, in the setting of no DSS feeding, *Mlkl*$^{-/-}$ mice compared with WT counterparts exhibited comparable amounts of myeloid cell populations (data not shown). Moreover, we detected considerably increased CD11b$^{+}$F4/80$^{+}$ cells in both spleen and LN of *Mlkl*$^{-/-}$ mice at day 5, thus indicating significantly increased inflammatory cell recruitment in response to injury (SFig. 3J and K). Similar results were observed in *Mlkl*$^{-/-}$ mice in the AOM + DSS-induced CAT model

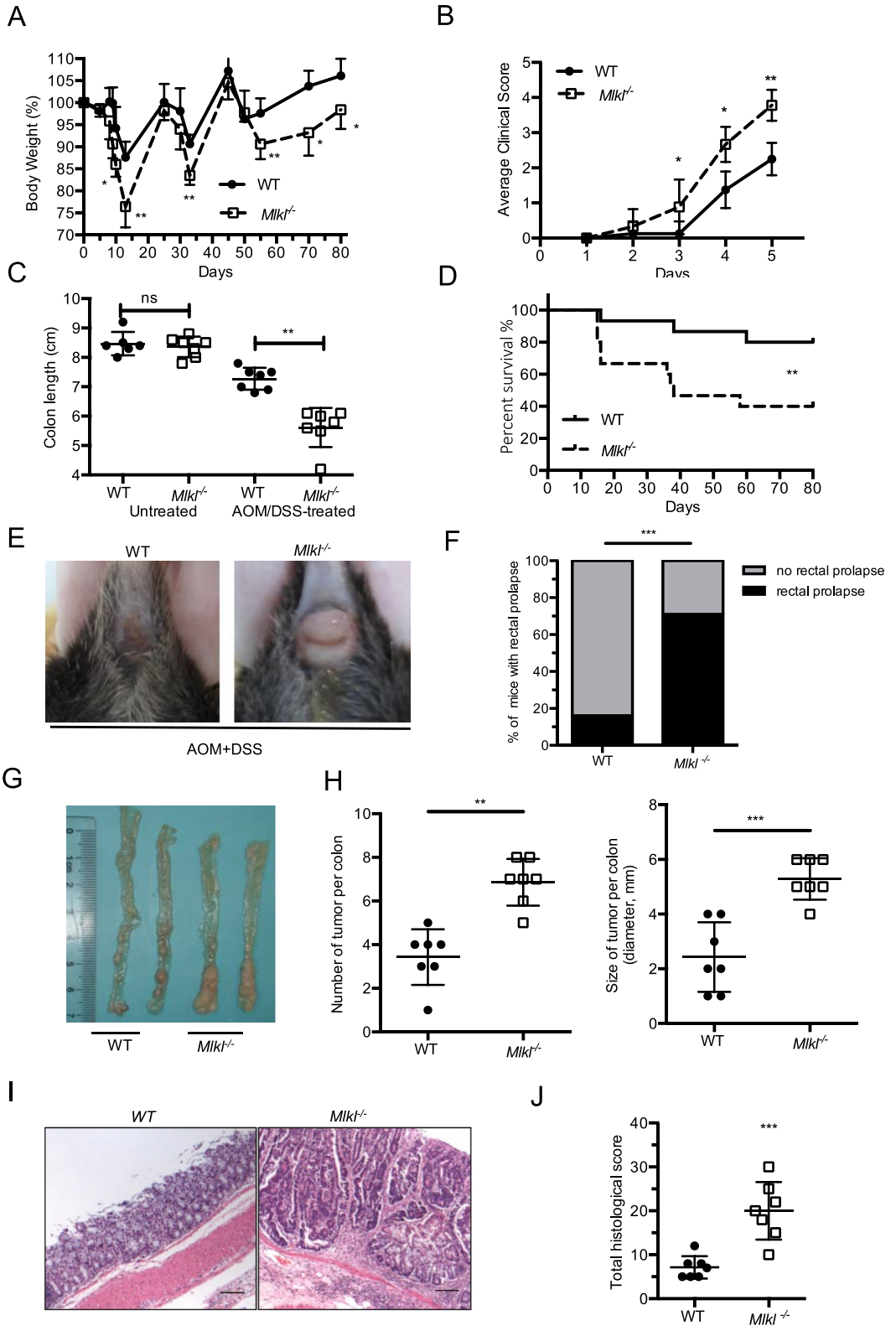


**Fig. 2. Increased colitis-associated tumorigenesis (CAT) in *Mlkl*$^{-/-}$ mice**. (A) Body weight changes were monitored after AOM/DSS treatment of WT (n = 15) and *Mlkl*$^{-/-}$ (n = 15) mice. (B) Rectal bleeding scores were determined after the 3rd DSS treatment cycle (C) Colons obtained from AOM/DSS-treated WT and *Mlkl*$^{-/-}$ mice.(D) Mice were monitored for survival in the AOM/DSS-induced CAT model.(E–F) Enhanced rectal prolapse in *Mlkl*$^{-/-}$ mice compared with WT mice on day 80.(G) Representative images of colonic tumor tissues from WT and *Mlkl*$^{-/-}$ mice at the end of the CAT model.(H) The number of tumors was counted and the size of tumors was measured in WT and *Mlkl*$^{-/-}$ mice. (I) Representative magnification images of colon polyps from WT and *Mlkl*$^{-/-}$ mice.(J) Histopathologic activity index (HAI) score in colons harvested from AOM/DSS-treated WT and *Mlkl*$^{-/-}$ mice. For all experiments, data shown are representative of at least three independent experiments. The symbols *, **and *** indicate $p < 0.05$, $p < 0.01$ and $p < 0.001$ respectively, between the AOM + DSS-treated WT and *Mlkl*$^{-/-}$ mice.

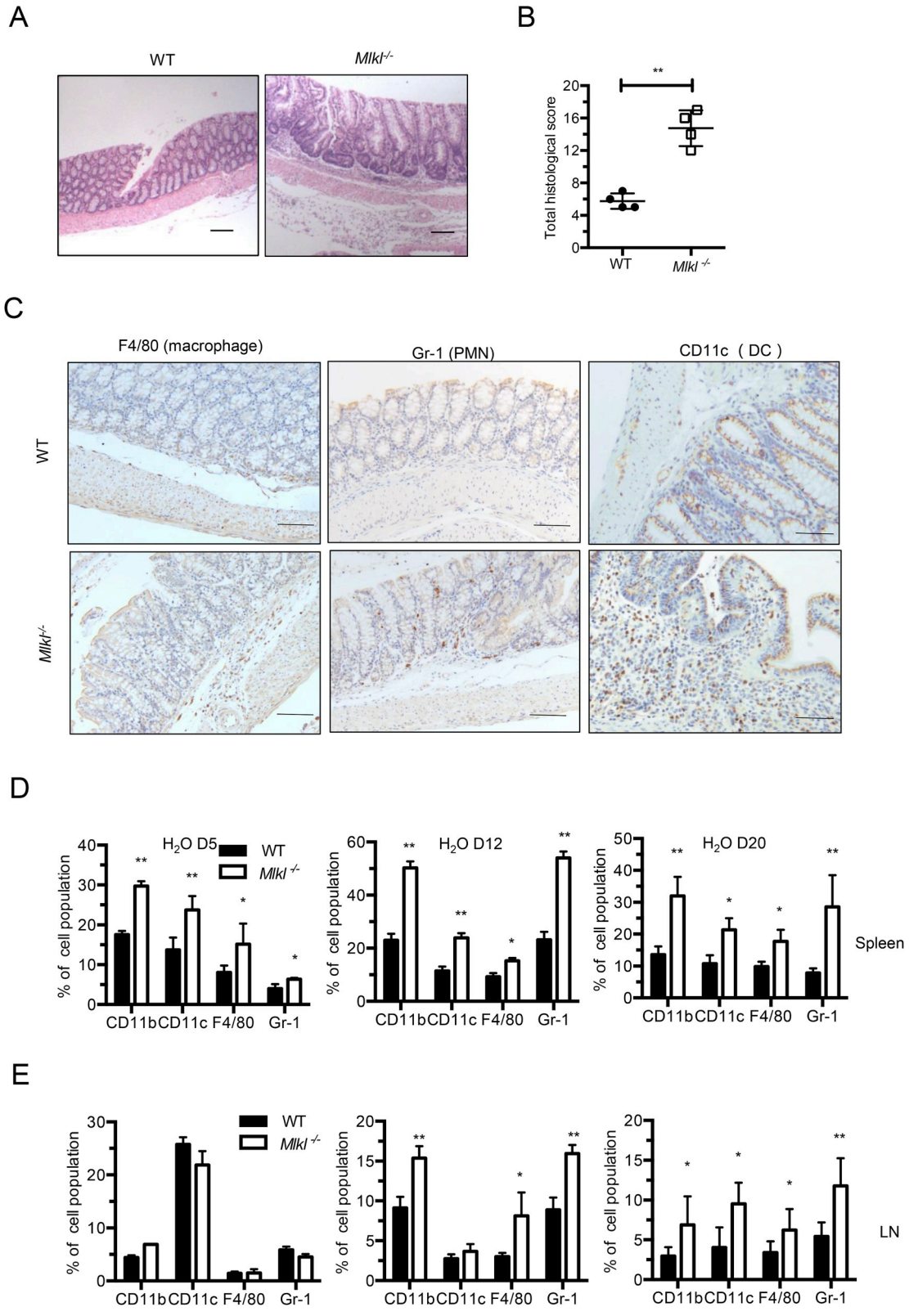


**Fig. 3. Exacerbated immune responses in *Mlkl*$^{-/-}$ mice during DSS exposure**. (A) Representative images of H&E-stained sections on day 15 after AOM injection (Normal water for 5 days).(B) Histopathologic activity index (HAI) score in colons at day 15 after AOM injection (Normal water for 5 days).(C) Colon tissue was immunostained for the macrophage marker F4/80, neutrophile marker Gr-1 and DC cells marker CD11c.(D–E) WT and *Mlkl*$^{-/-}$ mice were injected with AOM (Day 0). Five days later, mice were fed with 3% DSS for 5 days, followed by normal water for 5 days, 12 days and 20 days. Splenocytes (D) and mLN (E) cells were collected and analyzed by flow cytometry after staining for the myeloid cell population using CD11b, F4/80, CD11c and Gr-1 antibodies. The percentage of cell population at the indicated days. For all experiments, data shown are representative of at least three independent experiments. The symbols *, **and *** indicate $p < 0.05$, $p < 0.01$ and $p < 0.001$ respectively, between the AOM/DSS-treated WT and *Mlkl*$^{-/-}$ mice.

(SFig. 3L–N). Thus, these results collectively indicate that MLKL plays a critical role in reducing the inflammatory response during colitis and CAT.

### 3.4. Enhanced inflammatory response augments tumor-inducing factors in *Mlkl*$^{-/-}$ mice

Consistent with hyperactivation of myeloid cells in *Mlkl*$^{-/-}$ mice, the expression levels of proinflammatory cytokines (IL-1β, IL-6, TNF-α and IL17) and chemokines (G-CSF, eotaxin, KC, MCP-1) were prominently increased in the colons of *Mlkl*$^{-/-}$ mice compared with control mice at day 15 after AOM injection (SFig. 4A and B). Given the association of higher tumor burdens with higher production of proinflammatory cytokines and chemokines in AOM/DSS-treated *Mlkl*$^{-/-}$ mice, we detected increased proinflammatory cytokines and chemokines production in *Mlkl*$^{-/-}$ mice compared with WT mice in the context of the AOM/DSS-induced CAT model (SFig. 4C). Thus, these results suggest that *Mlkl*$^{-/-}$ mice exaggerate massive inflammatory responses during colitis and CAT.

To further understand the underlying mechanisms of inflammation and inflammation-induced tumorigenesis, we first analyzed the extent of the colonic mucosal epithelial cell proliferation and apoptosis after injury in *Mlkl*$^{-/-}$ mice. Interestingly, increased colonocyte proliferation as indicated by Ki67 staining was observed in hyperplastic colon regions of AOM/DSS-treated *Mlkl*$^{-/-}$ mice compared with WT mice (Fig. 4A). However, the number of TUNEL-positive cells in colons of *Mlkl*$^{-/-}$ mice was comparable with WT mice (Fig. 4B). In addition, increased expression of wound healing genes, such as Amphiregulin (Areg) and IL-11, were detected in *Mlkl*$^{-/-}$ mice compared with WT mice after being fed DSS. In addition, tissue remodeling genes, including metalloproteinase 10 (MMP-10) and COX-2, were also upregulated in *Mlkl*$^{-/-}$ mice. The relative expression of the antibacterial peptides Relmb was also increased, possibly in response to bacterial erosion into the colonic mucosa (Fig. 4C). The expression of inflammation and tumorigenic-associated genes is mediated by ERK, STAT3 and COX2 proteins. Consistent with the possibility of MLKL of reducing the activation of these signaling pathways, we observed significantly increased activation levels of ERK, STAT3 and COX2 in DSS-fed *Mlkl*$^{-/-}$ mice, which could potentially also drive the formation of colonic polyps (Fig. 4D and E). Taken together, above results indicate that DSS-treated *Mlkl*$^{-/-}$ mice create an inflammatory microenvironment upon exposure to DSS, leading to the development of colitis and tumorigenesis.

### 3.5. MLKL in immune cells is critical for protection against colitis

MLKL is ubiquitously expressed in bone marrow-derived immune cells and colonic tissue cells (SFig. 1E and F), which can function as suppressors in the development of colitis and CAT. To determine the likelihood that MLKL suppressed colitis and CAT development through directly regulating the function of inflammatory cells, bone marrow cells from WT and *Mlkl*$^{-/-}$ mice were transplanted into irradiated WT mice to generate chimeric mice (SFig. 5A). The bone marrow reconstitution efficiency was verified by transgenic allele-specific PCR from the chimeric mice (SFig. 5B). Two months after bone marrow reconstitution, mice were challenged with DSS as described above. As a result, WT mice receiving *Mlkl*$^{-/-}$ bone marrow (*Mlkl*$^{-/-}$ →WT) presented with severe colitis compared with WT mice transplanted with WT bone marrow (WT→WT). These effect was accompanied with increased weight loss and colitis severity (Fig. 5A and B), decreased colonic lengths and enlarged spleens (Fig. 5C **and** SFig. 5C and D). These clinical features of colitis were further confirmed by H&E staining (Fig. 5D). Consistent with the inflammatory responses, enhanced expression of inflammatory mediators was observed in *Mlkl*$^{-/-}$ →WT mice compared with WT→WT mice (SFig. 5E). Notably, increased activation of ERK and STAT3 was also detected in *Mlkl*$^{-/-}$ →WT mice (Fig. 5E and F). Taken together, these results suggest that MLKL in inflammatory cells is a potent protective role in colitis.

### 3.6. MLKL negatively regulates ERK activation and cytokine expression in DCs

Macrophages and DCs are critical immune defense cells that control inflammation through regulation of mediator and cytokine production [33]. To explore the evidence for inflammatory responses in *Mlkl*$^{-/-}$ mice, we used TLR4 ligand LPS and TLR3 ligand poly (I:C) to mimic stimulation of macrophages and DCs. Notably, ERK phosphorylation was increased in LPS-stimulated BMDCs from *Mlkl*$^{-/-}$ mice compared with WT mice (Fig. 6A **and** SFig. 6A). However, similar levels of NF-κB, p38 and JNK phosphorylation were noted in WT and *Mlkl*-deficient BMDC (SFig. 6B). Consistent with previously studies [29], *Mlkl* deficiency caused no markedly effect on LPS-induced activation of the NF-κB and MAPKs pathways in BMDMs (SFig. 6C). After Poly (I:C) stimulation, an increase in ERK phosphorylation was also observed in the *Mlkl*$^{-/-}$ BMDCs compared with WT mice but not in BMDMs (Fig. 6B **and** SFig. 6D). As our data indicated that Mlkl deficiency contributes to ERK activation, we next examined whether MLKL regulated the ERK cascades. ERK participate in the Ras-Raf-MEK-ERK signal transduction cascade [43]. LPS-induced phosphorylation of MEK was increased in *Mlkl*$^{-/-}$ BMDCs, but not in *Mlkl*$^{-/-}$ BMDMs (Fig. 6C **and** SFig. 6E). Interestingly, co-immunoprecipitation experiment showed that the interaction between ERK and MEK was enhanced in *Mlkl*$^{-/-}$ BMDCs (Fig. 6D). Correspondingly, expression of IL-1β, KC, MCP-1 and COX-2 was markedly increased in LPS-stimulated *Mlkl*$^{-/-}$ BMDCs but not in BMDMs (Fig. 6E **and** SFig. 6F and G).

To functionally examine the role of ERK as a potential down-stream effect molecule for MLKL deficiency-induced increasing of inflammatory responses, we further examined whether ERK inhibitor U0126 could affect the function of MLKL deficiency. Indeed, U0126 significantly inhibited LPS-induced ERK activation and cytokine expression by *Mlkl*$^{-/-}$ BMDCs (Fig. 6F and G). The similar set of experiments was also obtained after Poly (I:C) stimulation (Fig. 6H and I). By contrast, normal ammounts of cytokines in response to LPS or Poly (I:C) in *Mlkl*$^{-/-}$ BMDMs (SFig. 6H–K). In addition, overexpression of MLKL partially rescued the ERK activation and increased inflammatory cytokines in *Mlkl*$^{-/-}$ BMDCs (Fig. 6J). These data suggest that *Mlkl* deficiency might contribute to enhanced inflammatory responses in BMDCs by regulating MEK/ERK activation.

We next explored whether the increased inflammatory cytokines in *Mlkl*$^{-/-}$ BMDCs is associated with necroptosis. Compared to WT, *Mlkl*$^{-/-}$ BMDCs were resistant to necroptosis upon exposure to LPS or Poly (I:C) plus z-VAD (SFig. 7A–C). However, neither WT BMDCs nor *Mlkl*$^{-/-}$ BMDCs exhibited cell death in response to LPS or Poly (I:C) alone (SFig. 7A–C). RIPK3 is known to regulate the function of MLKL in the canonical necroptosis pathway. The expression of RIPK3 was unaffected in *Mlkl*$^{-/-}$ BMDCs (SFig. 7D and E). Moreover, RIPK3 knockdown did not contribution to ERK activation in *Mlkl*$^{-/-}$ BMDCs (SFig. 7F and 7G). To further explore the role of necroptosis in LPS-induced cytokine expression in BMDCs, we used RIPK1 kinase inhibitor Necrostatin-1 (Nec-1) and RIPK3-kinase inhibitor GSK′872. Nec-1 and GSK′872 significantly suppressed LPS + z-VAD-induced necroptosis (SFig. 7H), but did not affect ERK activation and LPS-induced cytokine expression in *Mlkl*$^{-/-}$ BMDCs (SFig. 7I and J).

We then determined whether necroptosis was contributing to the increased colitis and CAT in *Mlkl*$^{-/-}$ mice. Phosphorylation of S345 on MLKL has been demonstrated to be essential for canonical necroptotic cell death [31,44,45]. As shown in SFig. 7K, phosphorylation of MLKL was observed in WT BMDCs in response to LPS plus z-VAD. However, no phosphorylation of MLKL were presented in mucosal tissue during DSS-induced colitis. In addition, no phosphorylation of MLKL was detected in AOM + DSS-induced CAT model (**SFig. 7L**). These results indicated necroptosis does not contribute to the excessive inflammation

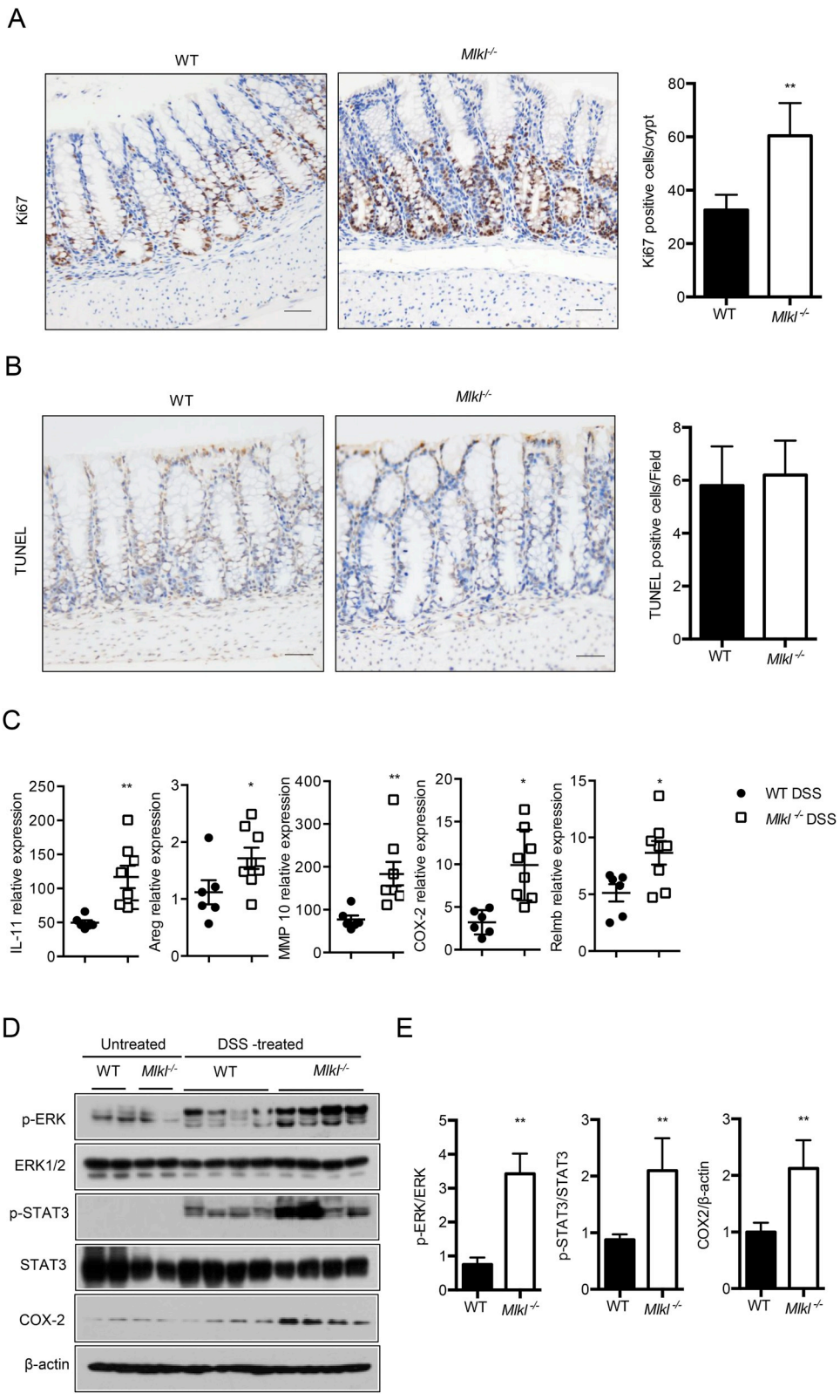


**Fig. 4. Enhanced inflammatory response augments tumor-inducing factors production in *Mlkl*$^{-/-}$ mice.** WT and *Mlkl*$^{-/-}$ mice were injected with AOM (Day 0). Five days later, mice were fed 3% DSS for 5 days followed by normal water for 5 days prior to euthanizing. (A–B) Immunohistochemical staining for Ki-67 and TUNEL from colon tissue of WT and *Mlkl*$^{-/-}$ mice. (C) The indicated gene expression profile in colon tissue was analyzed at day 15 after AOM + DSS treatment.(D) Whole colon tissue homogenates collected were examined for activation of ERK, STAT3 and COX2 expression by Western blot analysis. (E) Densitometric analysis was performed to determine the relative ratios of each protein.For all experiments, data shown are representative of at least three independent experiments. The symbols * and ** indicate $p < 0.05$ and $p < 0.01$ respectively, between the DSS-treated WT and *Mlkl*$^{-/-}$ mice.

in *Mlkl*-deficiency.

## 4. Discussion

MLKL is a commonly studied protein in necroptosis. Our results demonstrate that MLKL plays an important role in the suppression of proinflammatory cytokines and chemokines in colitis and CAT. Excessive inflammation in immune cells is critical for the development of colitis and CAT. Similarly, *Mlkl*$^{-/-}$ mice leads to increased susceptibility to colitis and CAT by hyperactivating the innate immune system. Intriguingly, MLKL in immune cells, likely contributed to the initiation of colitis. Furthermore, we show that MLKL control a necroptosis-independent pathway of inflammation through regulating cytokine expression in DCs. These data point to a currently

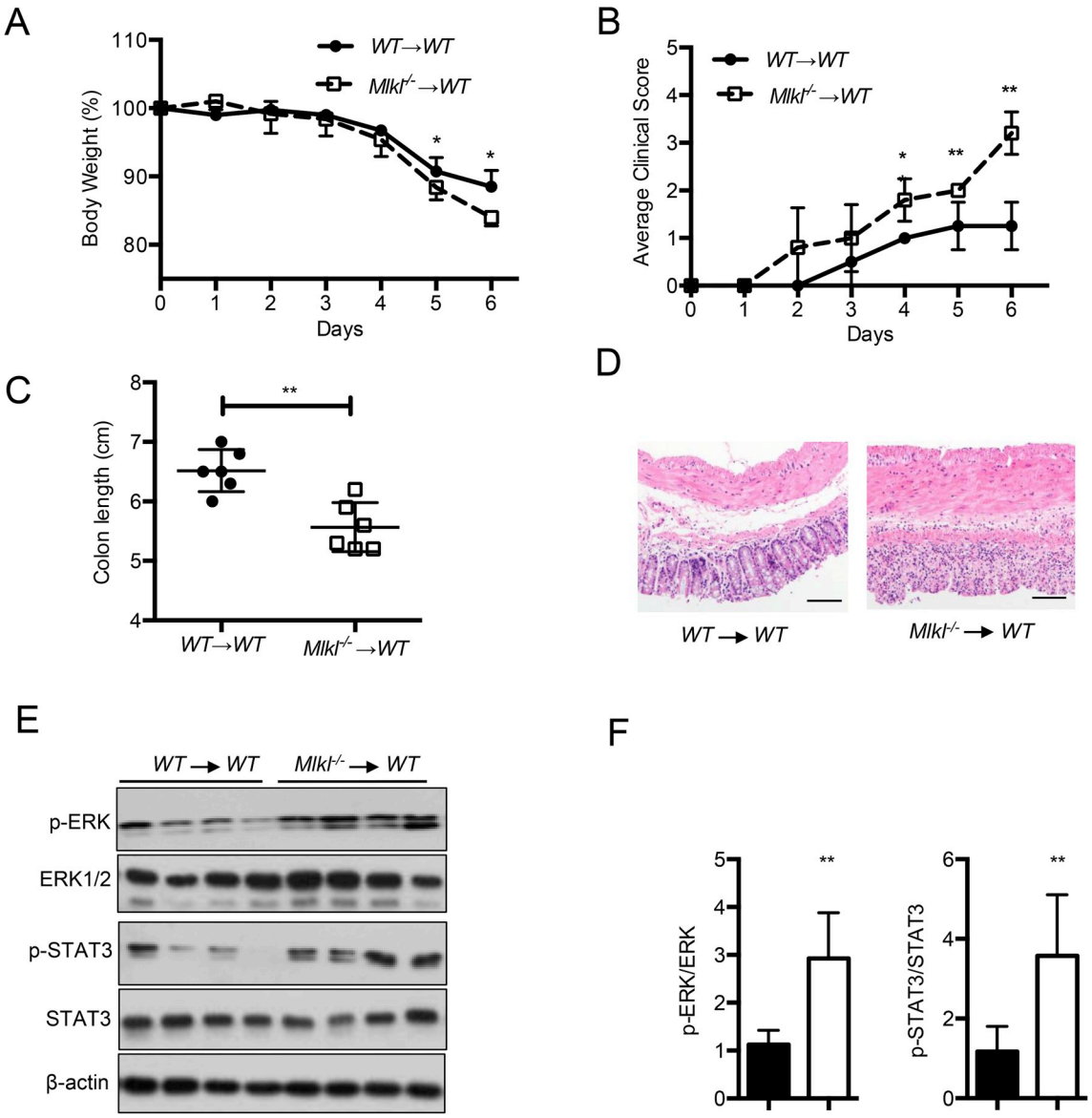


**Fig. 5. MLKL in immune cells is critical for protection against colitis and CAT.** (A–C) Bone marrow chimera mice for MLKL were generated (see Experimental Procedures). Eight weeks after, mice were induced colitis using DSS, respectively as described in the Experimental Procedures. WT (n = 6) and *Mlkl*$^{-/-}$ (n = 6) mice were treated with 3% DSS for 6 days. (A) Body weight, (B) average clinical scores and (C) colon length were monitored. (D) H&E-stained colon sections were examined and scored. (E–F) Whole colon tissue homogenates collected in bone marrow chimera mice were examined for activation of ERK, STAT3 and COX2 expression by Western blot analysis. Densitometric analysis was performed to determine the relative ratios of each protein. For all experiments, data shown are representative of at least three independent experiments. The symbols * and ** indicate $p < 0.05$ and $p < 0.01$, respectively, between the AOM/DSS-treated WT and *Mlkl*$^{-/-}$ mice.

unappreciated role for MLKL in promoting inflammation and CAT.

Inflammation is a dynamic process that requires molecular checkpoints to maintain immune homeostasis through tight regulation of inflammatory signaling pathways. However, several reports suggest that RIPK3 is critical for DSS-induced colitis and AOM/DSS-induced CAT independent of its function inducing cell death, independent of its function beyond inducing cell death [33,34]. In contrast, MLKL is well known as a key mediator of necroptosis [46]. However, the mechanism by which defective MLKL function is associated with hyperinflammatory responses in the colon remains unclear. The present study is distinguished by several unique features. First, *Mlkl*$^{-/-}$ mice are hypersusceptible to colon inflammation and CAT. Second, *Mlkl*$^{-/-}$ mice exhibited increased immune cell infiltration and hyperactivation of inflammatory responses in response to DSS treatment. Third, the link between overexpression of tumorigenic and proinflammatory genes and a number of key signaling pathways is well established [47,48]. Indeed, our data strongly support these concepts given that we observed that *Mlkl* deficiency can increased ERK, STAT3 and COX 2 activation, even in chimeric mice models. Our study provides evidence for anti-inflammatory role for MLKL by negatively regulating ERK signaling.

Interestingly, *Mlkl* deficiency in immune cells was critical for the progress of colitis and CAT. However, we could not exclude the possibility that MLKL might suppress immune responses in other cell types. Macrophages and DCs in the inflamed gut are important mediators in the response to immune inflammation during intestinal injury. In healthy controls, few intestinal DCs expressed TLR4, whereas DCs from inflamed tissue of patients with Crohn's disease are activated. In addition, the expression of microbial recognition receptors and pathologically relevant cytokines is up-regulated [49]. DSS-induced colitis is significantly more severe when DCs were selectively depleted in mice, suggesting that DCs are important for protection against colitis [50,51]. Our data indicate that MLKL regulates expression of specific set of

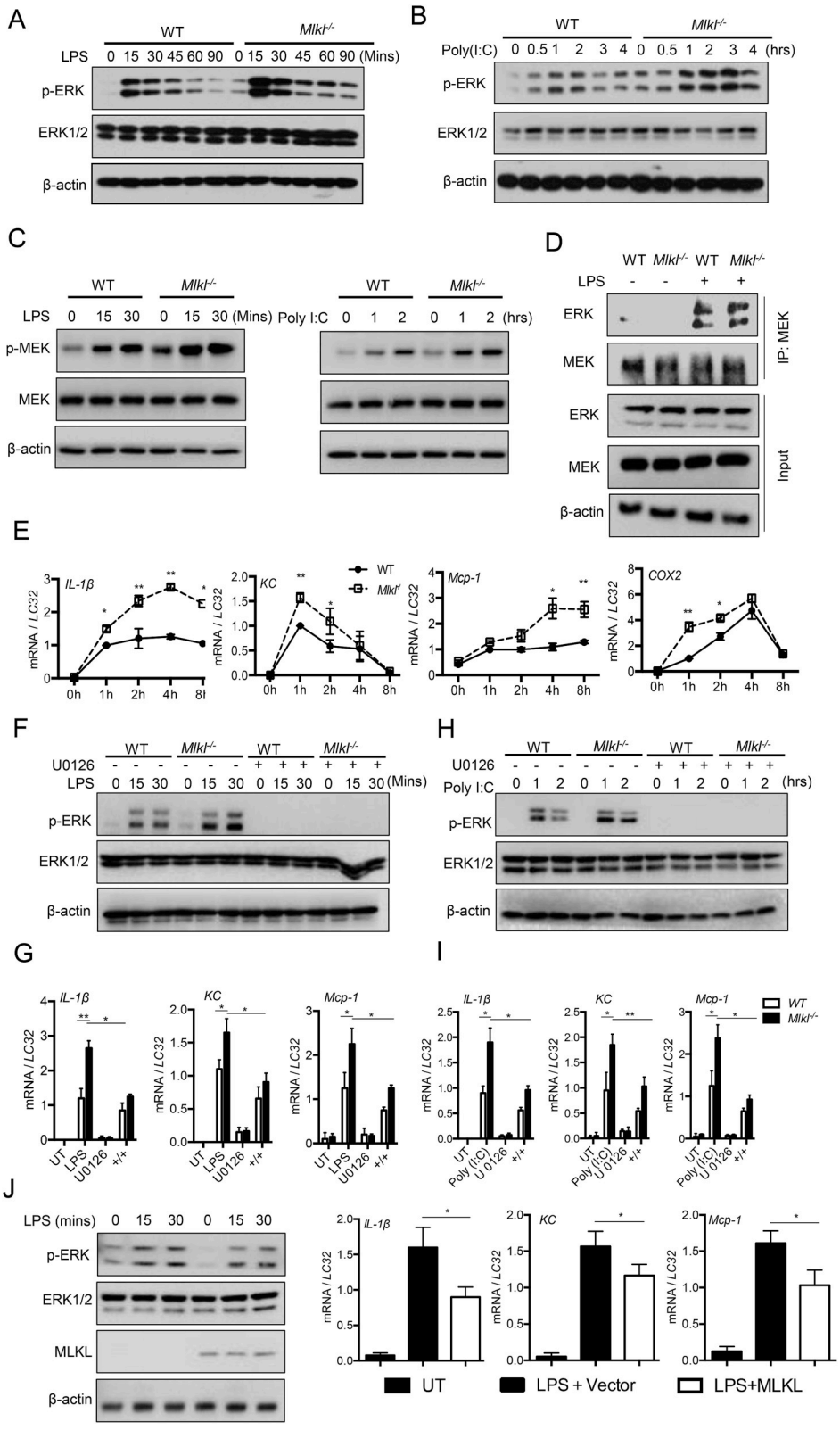


**Fig. 6. MLKL negatively regulate ERK activation and cytokine expression in DCs.** (A-B) BMDCs from WT and *Mlkl*$^{-/-}$ mice were stimulated with LPS (100 ng/ml) and poly (I:C) (100 μg/ml). Cell lysates harvested at indicated time points were analyzed for phospho-ERK, total ERK1/2 by Western blotting. (C) BMDCs from WT and *Mlkl*$^{-/-}$ mice were stimulated with LPS (100 ng/ml) for 15, 30 min and poly (I:C) (100 μg/ml) for 1, 2 h. Cell lysates harvested at indicated time points were analyzed for phospho-MEK, total MEK by Western blotting. (D) BMDCs from WT and *Mlkl*$^{-/-}$ mice were stimulated with LPS (100 ng/ml) for 15 min, and analyzed for the co-immunoprecipitation of MEK and ERK by Western blotting.(E) WT and *Mlkl*$^{-/-}$ BMDCs were stimulated with LPS (100 ng/ml) at the indicated time points, and mRNA was isolated for real-time PCR analysis.(F) WT and *Mlkl*$^{-/-}$ BMDCs were cultured in the presence of ERK inhibitor U0126 (10 μM), then stimulated with LPS as the indicated time points. Cell lysates were quantified for phospho-ERK, total ERK1/2, and β-actin by Western blots.(G) WT and *Mlkl*$^{-/-}$ BMDCs were cultured in the presence of ERK inhibitor U0126 (10 μM), then stimulated with LPS for 2 h. Cytokines expression was measured by real-time PCR.(H) WT and *Mlkl*$^{-/-}$ BMDCs were cultured in the presence of ERK inhibitor U0126 (10 μM), then stimulated with poly (I:C) as the indicated time points. Cell lysates were quantified for phospho-ERK, total ERK1/2, and β-actin by Western blots. (I) WT and *Mlkl*$^{-/-}$ BMDCs were cultured in the presence of ERK inhibitor U0126 (10 μM), then stimulated with poly (I:C). Cytokines expression was measured by real-time PCR.(J) *Mlkl*$^{-/-}$ BMDCs were infected with viruses encoding MLKL or vector for 48 h, and then stimulated with LPS, following to evaluate the levels of phospho-ERK by immunoblot. Cytokines expression was measured by real-time PCR.All data shown are representative of at least three independent experiments. The symbols * and ** indicate $p < 0.05$ and $p < 0.01$ respectively.

cytokine expression in *Mlkl*$^{-/-}$ BMDCs, but not BMDMs, via regulating ERK activation. Further investigation is needed to clearly determine why *Mlkl*-deficiency exhibit different effect on DCs and macrophages. Our data indicated that MLKL regulates expression of specific set of cytokine expression via regulating MEK/ERK activation, in *Mlkl*$^{-/-}$ BMDCs, but not BMDMs. U0126 suppressed the LPS-induced cytokine expression in *Mlkl*$^{-/-}$ BMDCs, while overexpression of MLKL resulted in an opposing effect. Although our results suggested a role for *Mlkl*-deficiency in the association between MEK and ERK, the mechanisms of MLKL in MEK/ERK signaling cascades is not yet clear and need to be further investigated in the future.

As a substrate of RIPK3, MLKL is essential for necroptosis. Recent studies has revealed that necroptosis exhibited proinflammatory and anti-inflammatory effects in certain settings [52,53]. Given this

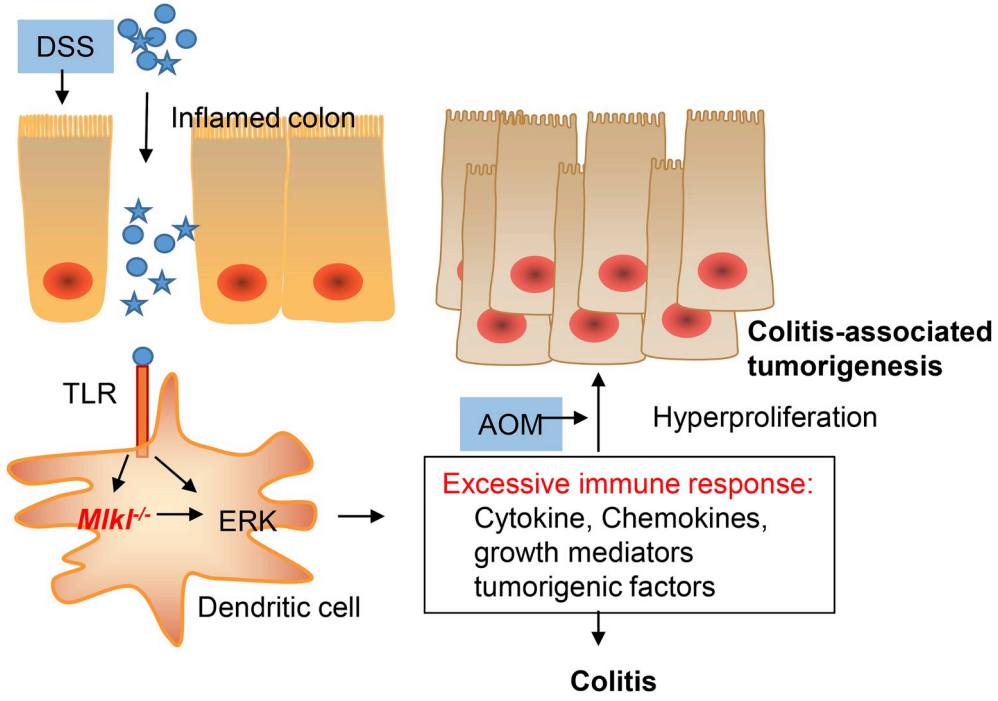


**Fig. 7.** A proposed model for MLKL participating in colon inflammation and colitis-associated tumorigenesis.

relationship, one might hypothesize that necroptosis and RIPK3 are responsible for the increased inflammation during colitis. However, in our study, we did not observe that MLKL was phosphorylated during DSS-induced colitis. In addition, LPS alone was not sufficient to induce cell death in WT and *Mlkl*$^{-/-}$ BMDCs. Moreover, necroptosis inhibitors also did not affect LPS-induced cytokine expression. Therefore, these data suggest that MLKL display divergent roles beyond necroptosis during colitis injury and function independently of each other, which is supported by our previous findings and studies conducted by others [35,36].

In conclusion, our findings provide strong evidence for anti-inflammatory and anti-tumor role of MLKL *in vivo* through negatively ERK signaling (Fig. 7). In addition, we uncover that the role of MLKL might determine not only in necroptosis, but also in cytokine responses by various stimulus.

## Authorship contributions

Q.Z, X.J.Y and H.B.Z designed the study and planned the experiment. Q.Z and X.J.Y performed the experiment and analyzed data with assistance from other authors. H.B.Z supervised project and together with Q.Z and X.J.Y wrote the manuscript.

## Conflicts of interest

The authors declare that they have no competing interests.

## Disclosures

The authors have no financial conflicts of interest.

## Acknowledgements

This work was supported by grants from the National Natural Science Foundation of China (31571426, 81502548, 31670785), the Ministry of Science and Technology of the People's Republic of China (2016YFC1304900 and 2018YFC1200201), the Cultivating Project for Young Scholar at Hubei University of Medicine (2018QDJZR06) and the Biomedical Research Foundation, Hubei University of Medicine (HBMUPI201809).

## Appendix A. Supplementary data

Supplementary data to this article can be found online at https://doi.org/10.1016/j.canlet.2019.05.034.

## References

[1] S.M. Laster, J.G. Wood, L.R. Gooding, Tumor necrosis factor can induce both apoptic and necrotic forms of cell-lysis, J. Immunol. 141 (1988) 2629–2634.
[2] R. Medzhitov, Origin and physiological roles of inflammation, Nature 454 (2008) 428–435.
[3] S.I. Grivennikov, F.R. Greten, M. Karin, Immunity, inflammation, and cancer, Cell 140 (2010) 883–899.
[4] R.L. Siegel, K.D. Miller, A. Jemal, Cancer statistics, Ca - Cancer J. Clin. 67 (2017) (2017) 7–30.
[5] W.Q. Chen, R.S. Zheng, P.D. Baade, S.W. Zhang, H.M. Zeng, F. Bray, A. Jemal, X.Q. Yu, J. He, Cancer statistics in China, 2015, Ca - Cancer J. Clin. 66 (2016) 115–132.
[6] J.A. Eaden, K.R. Abrams, J.F. Mayberry, The risk of colorectal cancer in ulcerative colitis: a meta-analysis, Gut 48 (2001) 526–535.
[7] L.A. Feagins, R.F. Souza, S.J. Spechler, Carcinogenesis in IBD: potential targets for the prevention of colorectal cancer, Nat. Rev. Gastroenterol. Hepatol. 6 (2009) 297–305.
[8] C. Canavan, K.R. Abrams, J. Mayberry, Meta-analysis: colorectal and small bowel cancer risk in patients with Crohn's disease, Aliment Pharmacol. Ther. 23 (2006) 1097–1104.
[9] P. Goyette, C. Labbe, T.T. Trinh, R.J. Xavier, J.D. Rioux, Molecular pathogenesis of inflammatory bowel disease: genotypes, phenotypes and personalized medicine, Ann. Med. 39 (2007) 177–199.
[10] W. Strober, I.J. Fuss, R.S. Blumberg, The immunology of mucosal models of inflammation, Annu. Rev. Immunol. 20 (2002) 495–549.
[11] S.U. Seo, N. Kamada, R. Munoz-Planillo, Y.G. Kim, D. Kim, Y. Koizumi, M. Hasegawa, S.D. Himpsl, H.P. Browne, T.D. Lawley, H.L.T. Mobley, N. Inohara, G. Nunez, Distinct commensals induce interleukin-1 beta via NLRP3 inflammasome in inflammatory monocytes to promote intestinal inflammation in response to injury, Immunity 42 (2015) 744–755.
[12] J. Dupaul-Chicoine, G. Yeretssian, K. Doiron, K.S.B. Bergstrom, C.R. McIntire, P.M. LeBlanc, C. Meunier, C. Turbide, P. Gros, N. Beauchemin, B.A. Vallance, M. Saleh, Control of intestinal homeostasis, colitis, and colitis-associated colorectal cancer by the inflammatory caspases, Immunity 32 (2010) 367–378.
[13] M.H. Zaki, P. Vogel, R.K. Malireddi, M. Body-Malapel, P.K. Anand, J. Bertin, D.R. Green, M. Lamkanfi, T.D. Kanneganti, The NOD-like receptor NLRP12 attenuates colon inflammation and tumorigenesis, Cancer Cell 20 (2011) 649–660.
[14] C.M. Leu, F.H. Wong, C.M. Chang, S.F. Huang, C.P. Hu, Interleukin-6 acts as an

antiapoptotic factor in human esophageal carcinoma cells through the activation of both STAT3 and mitogen-activated protein kinase pathways, Oncogene 22 (2003) 7809–7818.
[15] C. van Vliet, P.E. Bukczynska, M.A. Puryer, C.M. Sadek, B.J. Shields, M.L. Tremblay, T. Tiganis, Selective regulation of tumor necrosis factor-induced Erk signaling by Src family kinases and the T cell protein tyrosine phosphatase, Nat. Immunol. 6 (2005) 253–260.
[16] I.C. Allen, J.E. Wilson, M. Schneider, J.D. Lich, R.A. Roberts, J.C. Arthur, R.M.T. Woodford, B.K. Davis, J.M. Uronis, H.H. Herfarth, C. Jobin, A.B. Rogers, J.P.Y. Ting, NLRP12 suppresses colon inflammation and tumorigenesis through the negative regulation of noncanonical NF-kappa B signaling, Immunity 36 (2012) 742–754.
[17] H. Lee, A. Herrmann, J.H. Deng, M. Kujawski, G.L. Niu, Z.W. Li, S. Forman, R. Jove, D.M. Pardoll, H. Yu, Persistently activated Stat3 maintains constitutive NF-kappa B activity in tumors, Cancer Cell 15 (2009) 283–293.
[18] H. Yu, M. Kortylewski, D. Pardoll, Crosstalk between cancer and immune cells: role of STAT3 in the tumour microenvironment, Nat. Rev. Immunol. 7 (2007) 41–51.
[19] X. Ma, Z. Meng, L. Jin, Z. Xiao, X. Wang, W.M. Tsark, L. Ding, Y. Gu, J. Zhang, B. Kim, M. He, X. Gan, J.E. Shively, H. Yu, R. Xu, W. Huang, CAMK2gamma in intestinal epithelial cells modulates colitis-associated colorectal carcinogenesis via enhancing STAT3 activation, Oncogene 36 (2017) 4060–4071.
[20] M. Kohno, J. Pouyssegur, Targeting the ERK signaling pathway in cancer therapy, Ann. Med. 38 (2006) 200–211.
[21] E.F. Wagner, A.R. Nebreda, Signal integration by JNK and p38 MAPK pathways in cancer development, Nat. Rev. Canc. 9 (2009) 537–549.
[22] C.A. Singer, K.J. Baker, A. McCaffrey, D.P. AuCoin, M.A. Dechert, W.T. Gerthoffer, p38 MAPK and NF-kappa B mediate COX-2 expression in human airway myocytes, Am. J. Physiol.-Lung C 285 (2003) L1087–L1098.
[23] F.K. Chan, J. Shisler, J.G. Bixby, M. Felices, L. Zheng, M. Appel, J. Orenstein, B. Moss, M.J. Lenardo, A role for tumor necrosis factor receptor-2 and receptor-interacting protein in programmed necrosis and antiviral responses, J. Biol. Chem. 278 (2003) 51613–51621.
[24] N. Holler, R. Zaru, O. Micheau, M. Thome, A. Attinger, S. Valitutti, J.L. Bodmer, P. Schneider, B. Seed, J. Tschopp, Fas triggers an alternative, caspase-8-independent cell death pathway using the kinase RIP as effector molecule, Nat. Immunol. 1 (2000) 489–495.
[25] Y. Cho, S. Challa, D. Moquin, R. Genga, T.D. Ray, M. Guildford, F.K.M. Chan, Phosphorylation-driven assembly of the RIP1-RIP3 complex regulates programmed necrosis and virus-induced inflammation, Cell 137 (2009) 1112–1123.
[26] S.D. He, L. Wang, L. Miao, T. Wang, F.H. Du, L.P. Zhao, X.D. Wang, Receptor interacting protein kinase-3 determines cellular necrotic response to TNF-alpha, Cell 137 (2009) 1100–1111.
[27] L.M. Sun, H.Y. Wang, Z.G. Wang, S.D. He, S. Chen, D.H. Liao, L. Wang, J.C. Yan, W.L. Liu, X.G. Lei, X.D. Wang, Mixed lineage kinase domain-like protein mediates necrosis signaling downstream of RIP3 kinase, Cell 148 (2012) 213–227.
[28] S. Yoon, A. Kovalenko, K. Bogdanov, D. Wallach, MLKL, the protein that mediates necroptosis, also regulates endosomal trafficking and extracellular vesicle generation, Immunity 47 (2017) 51–+.
[29] J.F. Wu, Z. Huang, J.M. Ren, Z.R. Zhang, P. He, Y.X. Li, J.H. Ma, W.Z. Chen, Y.Y. Zhang, X.J. Zhou, Z.T. Yang, S.Q. Wu, L.F. Chen, J.H. Han, Mlkl knockout mice demonstrate the indispensable role of Mlkl in necroptosis, Cell Res. 23 (2013) 994–1006.
[30] I. Tabas, Macrophage death and defective inflammation resolution in atherosclerosis, Nat. Rev. Immunol. 10 (2010) 36–46.
[31] Q. Zhao, X. Yu, H. Zhang, Y. Liu, X. Zhang, X. Wu, Q. Xie, M. Li, H. Ying, RIPK3 mediates necroptosis during embryonic development and postnatal inflammation in fadd-deficient mice, Cell Rep. 19 (2017) 798–808.
[32] K. Kitur, S. Wachtel, A. Brown, M. Wickersham, F. Paulino, H.F. Penaloza, G. Soong, S. Bueno, D. Parker, A. Prince, Necroptosis promotes Staphylococcus aureus clearance by inhibiting excessive inflammatory signaling, Cell Rep. 16 (2016) 2219–2230.
[33] K. Moriwaki, S. Balaji, T. McQuade, N. Malhotra, J. Kang, F.K. Chan, The necroptosis adaptor RIPK3 promotes injury-induced cytokine expression and tissue repair, Immunity 41 (2014) 567–578.
[34] G. Yan, H. Zhao, Q. Zhang, Y. Zhou, L. Wu, J. Lei, X. Wang, J. Zhang, X. Zhang, L. Zheng, G. Du, W. Xiao, B. Tang, H. Miao, Y. Li, A RIPK3-PGE2 circuit mediates myeloid-derived suppressor cell-potentiated colorectal carcinogenesis, Cancer Res. 78 (2018) 5586–5599.
[35] S. Alvarez-Diaz, C.P. Dillon, N. Lalaoui, M.C. Tanzer, D.A. Rodriguez, A. Lin, M. Lebois, R. Hakem, E.C. Josefsson, L.A. O'Reilly, J. Silke, W.S. Alexander, D.R. Green, A. Strasser, The pseudokinase MLKL and the kinase RIPK3 have distinct roles in autoimmune disease caused by loss of death-receptor-induced apoptosis, Immunity 45 (2016) 513–526.
[36] X. Zhang, C. Fan, H. Zhang, Q. Zhao, Y. Liu, C. Xu, Q. Xie, X. Wu, X. Yu, J. Zhang, MLKL and FADD are critical for suppressing progressive lymphoproliferative disease and activating the NLRP3 inflammasome, Cell Rep. 16 (2016) 3247–3259.
[37] L. Van Hoecke, S. Van Lint, K. Roose, A. Van Parys, P. Vandenabeele, J. Grooten, J. Tavernier, S. De Koker, X. Saelens, Treatment with mRNA coding for the necroptosis mediator MLKL induces antitumor immunity directed against neo-epitopes, Nat. Commun. 9 (2018) 3417.
[38] X. Li, J. Guo, A.P. Ding, W.W. Qi, P.H. Zhang, J. Lv, W.S. Qiu, Z.Q. Sun, Association of mixed lineage kinase domain-like protein expression with prognosis in patients with colon cancer, Technol. Canc. Res. Treat. 16 (2017) 428–434.
[39] A.L. Hart, H.O. Al-Hassi, R.J. Rigby, S.J. Bell, A.V. Emmanuel, S.C. Knight, M.A. Kamm, A.J. Stagg, Characteristics of intestinal dendritic cells in inflammatory bowel diseases, Gastroenterology 129 (2005) 50–65.
[40] X.J. Yu, Q.B. Han, Z.S. Wen, L. Ma, J. Gao, G.B. Zhou, Gambogenic acid induces G1 arrest via GSK3beta-dependent cyclin D1 degradation and triggers autophagy in lung cancer cells, Cancer Lett. 322 (2012) 185–194.
[41] J. Zhao, S. Jitkaew, Z.Y. Cai, S. Choksi, Q.N. Li, J. Luo, Z.G. Liu, Mixed lineage kinase domain-like is a key receptor interacting protein 3 downstream component of TNF-induced necrosis, P Natl Acad Sci USA 109 (2012) 5322–5327.
[42] Y.F. Liu, J.J. Peng, T.Y. Sun, N. Li, L. Zhang, J.L. Ren, H.R. Yuan, S. Kan, Q. Pan, X. Li, Y.F. Ding, M. Jiang, X.J. Cong, M.J. Tan, Y.S. Ma, D. Fu, S.J. Cai, Y.C. Xiao, X.M. Wang, J. Qin, Epithelial EZH2 serves as an epigenetic determinant in experimental colitis by inhibiting TNF alpha-mediated inflammation and apoptosis, P Natl Acad Sci USA 114 (2017) E3796–E3805.
[43] R. Roskoski Jr., ERK1/2 MAP kinases: structure, function, and regulation, Pharmacol. Res. 66 (2012) 105–143.
[44] M.C. Tanzer, A. Tripaydonis, A.I. Webb, S.N. Young, L.N. Varghese, C. Hall, W.S. Alexander, J.M. Hildebrand, J. Silke, J.M. Murphy, Necroptosis signalling is tuned by phosphorylation of MLKL residues outside the pseudokinase domain activation loop, Biochem. J. 471 (2015) 255–265.
[45] C. Gunther, G.W. He, A.E. Kremer, J.M. Murphy, E.J. Petrie, K. Amann, P. Vandenabeele, A. Linkermann, C. Poremba, U. Schleicher, C. Dewitz, S. Krautwald, M.F. Neurath, C. Becker, S. Wirtz, The pseudokinase MLKL mediates programmed hepatocellular necrosis independently of RIPK3 during hepatitis, J. Clin. Investig. 126 (2016) 4346–4360.
[46] J.M. Murphy, P.E. Czabotar, J.M. Hildebrand, I.S. Lucet, J.G. Zhang, S. Alvarez-Diaz, R. Lewis, N. Lalaoui, D. Metcalf, A.I. Webb, S.N. Young, L.N. Varghese, G.M. Tannahill, E.C. Hatchell, I.J. Majewski, T. Okamoto, R.C.J. Dobson, D.J. Hilton, J.J. Babon, N.A. Nicola, A. Strasser, J. Silke, W.S. Alexander, The pseudokinase MLKL mediates necroptosis via a molecular switch mechanism, Immunity 39 (2013) 443–453.
[47] L.M. Coussens, Z. Werb, Inflammation and cancer, Nature 420 (2002) 860–867.
[48] Y. Grinberg-Bleyer, S. Ghosh, A novel link between inflammation and cancer, Cancer Cell 30 (2016) 829–830.
[49] M.C. Bonnet, D. Preukschat, P.S. Welz, G. van Loo, M.A. Ermolaeva, W. Bloch, I. Haase, M. Pasparakis, The adaptor protein FADD protects epidermal keratinocytes from necroptosis in vivo and prevents skin inflammation, Immunity 35 (2011) 572–582.
[50] P.S. Welz, A. Wullaert, K. Vlantis, V. Kondylis, V. Fernandez-Majada, M. Ermolaeva, P. Kirsch, A. Sterner-Kock, G. van Loo, M. Pasparakis, FADD prevents RIP3-mediated epithelial cell necrosis and chronic intestinal inflammation, Nature 477 (2011) 330-U102.
[51] J.E. Qualls, H. Tuna, A.M. Kaplan, D.A. Cohen, Suppression of experimental colitis in mice by CDllc(+) dendritic cells, Inflamm. Bowel Dis. 15 (2009) 236–247.
[52] C.J. Kearney, S.P. Cullen, G.A. Tynan, C.M. Henry, D. Clancy, E.C. Lavelle, S.J. Martin, Necroptosis suppresses inflammation via termination of TNF- or LPS-induced cytokine and chemokine production, Cell Death Differ. 22 (2015) 1313–1327.
[53] M. Pasparakis, P. Vandenabeele, Necroptosis and its role in inflammation, Nature 517 (2015) 311–320.